Consequences of Proposed Shoreline Deformation Scenarios for Jezero Crater, Mars

Mark Baum[1] , Robin Wordsworth[1,2] , and Timothy A. Goudge[3]
[1] Department of Earth and Planetary Sciences, Harvard University, Cambridge, MA 02138, USA; markbaum@g.harvard.edu
[2] Paulson School of Engineering and Applied Sciences, Harvard University, Cambridge, MA 02138, USA
[3] Jackson School of Geosciences, The University of Texas at Austin, Austin, TX 78712, USA

Abstract

One of the most interesting questions about the climate and hydrology of early Mars is whether oceans existed and, if so, when. Various geologic features have been interpreted as ancient shorelines, but these features do not follow gravitational equipotentials. Prior work has shown that the elevation of the Arabia level, hypothesized to represent a large, early ocean, better conforms to an equipotential when correcting for global topographic change after its formation. Although the shoreline coordinates underlying these studies are debated, exploring the consequences of these topographic corrections allows additional observable consequences to be identified. Here we show that the topographic corrections cause Jezero crater, the landing site of the Perseverance rover, to be submerged under the proposed Arabia ocean. This precludes the ocean's existence during known fluvio-lacustrine activity at Jezero and suggests the ocean did not exist during the main era of valley network formation in the Noachian/Early Hesperian. We identify a period of $\sim 10^8$ yr years before fluvial activity at Jezero when the ocean could have existed and discuss potential observable consequences.

Unified Astronomy Thesaurus concepts: Mars (1007)

1. Introduction

The nature of the early Martian climate is a long-standing enigma in planetary science. Today, the surface of Mars is dry and frozen, but in the distant past, it hosted more temperate environments. Large valley networks, lacustrine deltas, fluvial conglomerates, and other features are preserved on the oldest regions of the Martian surface (Malin & Edgett 2003; Fassett & Head 2008a; Hynek et al. 2010; Williams et al. 2013; Grotzinger et al. 2015), clear evidence of an active water cycle more than 3 billion years ago. A body of water roughly half the size of Earth's Mediterranean appears to have existed on the surface (Irwin et al. 2002) and there may have been even larger seas (Moore & Wilhelms 2001; Grant & Parker 2002). This evidence is mysterious because, given the planet's orbital distance and a fainter young Sun, early Mars should have been cold. Although the early atmosphere was probably much thicker, a hierarchy of climate models has demonstrated that a CO_2–H_2O greenhouse alone could not have achieved warm and wet conditions (Kasting 1991; Wordsworth et al. 2010; Forget et al. 2013; Urata & Toon 2013; Wordsworth et al. 2013; Soto et al. 2015; Steakley et al. 2019).

One of the most interesting questions about early Martian climate and hydrology is whether large oceans ever covered the northern lowlands on Mars. From the 1980s onward, analysis of satellite images led to proposals that various geologic features are markers of an ancient ocean's shoreline (Parker et al. 1989, 1993). Although many landforms have been discussed, including deltas and valley network termini (Di Achille & Hynek 2010; Chan et al. 2018), most work has focused on the Arabia and Deuteronilus levels, curvilinear features around the hemispheric dichotomy. These levels are hypothesized to represent an older, larger ocean and a younger,

smaller ocean, respectively (Head et al. 1999). However, the modern elevation of these features varies significantly, implying they could not have been created by a level body of water with present Martian topography (Carr & Head 2003). The older Arabia level, in particular, exhibits long-wavelength elevation variation of several kilometers and a great deal of scatter over shorter distances (Head et al. 1999; Carr & Head 2003). Recognizing this, several studies have investigated the potential role of global topographic modification after formation of the putative shorelines. Thermal isostasy and lithospheric flexure under the ocean's load have both been considered (Leverington & Ghent 2004; Ruiz et al. 2004), although without specific models correcting the variation in putative shoreline elevations. More recently, investigations of topographic change in response to true polar wander (TPW) and the rise of the Tharsis volcanic province have been proposed with specific topographic correction scenarios (Perron et al. 2007; Citron et al. 2018).

In addition to the elevation variation of the proposed paleoshorelines, ocean hypotheses are complicated by several other issues (Head et al. 2018). First, further examination of the features with higher-resolution images has called the shoreline interpretation directly into question (Malin & Edgett 1999; Sholes et al. 2014, 2019a, 2019b, 2021). Second, the proposed shorelines are often poorly defined. The Arabia level, in particular, has been mapped differently in various studies and lacks a standard set of coordinates (Sholes et al. 2021). Third, climate modeling suggests that unless the planet was strongly and continuously warmed, ocean water would have migrated to high-elevation and polar cold traps to form large ice sheets and glaciers (Wordsworth et al. 2013; Wordsworth 2016; Turbet & Forget 2019). This is important, as several lines of evidence argue against a warm and wet early climate enduring for more than 10^7 yrs. The abundance of unaltered ancient igneous minerals, relative absence of carbonates, and nature of many observed phyllosilicates (Ehlmann et al. 2011; Niles et al. 2013; Ehlmann & Edwards 2014; Bishop et al. 2018) are most

consistent with a mainly cold climate with only brief warm periods. While geomorphic studies indicate that between 10^4 and 10^7 years of active surface hydrology are needed to erode the valley networks and deposit sediments in craters (Hoke et al. 2011; Grotzinger et al. 2014), this is a small fraction of the 10^8–10^9 yr duration of early Martian history spanning the Noachian and Early Hesperian.

All of these considerations make the existence of early, long-lived Martian oceans difficult to justify. However, there is still much that is unknown about early Mars, and early oceans must be investigated in the context of our improving understanding of early Martian environments. Confirmation or contradiction of the ocean hypotheses would constrain the early Martian climate, near-surface water inventory, and habitability, which in turn affects the question of whether life arose on Mars. Continued investigation of this question is important.

Here we link hypotheses for an early Arabia ocean, and the subsequent deformation of its paleoshoreline, to the geology of Jezero crater, the landing site for NASA's Perseverance rover (Mars 2020). In Section 2, we review how two previous studies have attempted to explain the elevation variation of the Arabia level with global topographic deformation models and reproduce these results. In Section 3, we apply the topographic deformation models to the region around Jezero and examine how the proposed ocean would impact this area. In Section 4, we discuss implications for the timing of the proposed ocean, including whether they could have coincided with the main era of global valley network activity during the Noachian/Early Hesperian (Howard et al. 2005; Irwin et al. 2005; Fassett & Head 2008b; Hynek et al. 2010).

2. Global Topography and the Arabia Level

Two studies explained the modern elevation variation of proposed paleoshorelines by correcting for topographic change after their formation. Here we refer to them as the "true polar wander (TPW) scenario" and the "Tharsis growth scenario." First, Perron et al. (2007) proposed the TPW scenario, where deformation in response to a rotated gravitational potential flattened the Arabia level. In this scenario, the Arabia level formed relatively late, after most of the Tharsis rise was constructed. More recently, Citron et al. (2018) proposed the Tharsis growth scenario, in which deformation due to the formation of Tharsis itself, not TPW, caused the elevation variation of the Arabia level. In their scenario, the Arabia level must have formed before most of Tharsis was constructed, likely >3.7 Ga (Anderson et al. 2001).

The TPW scenario relies on internal mass loading associated with mantle convection to drive the required polar shift. This is because most evidence indicates Tharsis formed near the equator (Roberts & Zhong 2007; Daradich et al. 2008; Matsuyama & Manga 2010; Bouley et al. 2016) and drove relatively little TPW, so surface mass loads would be insufficient to drive the necessary TPW (Perron et al. 2007; Citron et al. 2018). The Tharsis growth scenario, on the other hand, only depends on a clearly identifiable load (Tharsis) to drive topographic deformation. Hence, the Tharsis growth scenario is better geophysically grounded. However, neither of the two corrections flatten the Arabia level completely (see Figure 1 of this paper, Figure 1(b) of Perron et al. 2007, and Figure 1(b) of Citron et al. 2018), and one study favors the TPW scenario on the basis of independent analysis of valley network termini locations Chan et al. (2018).
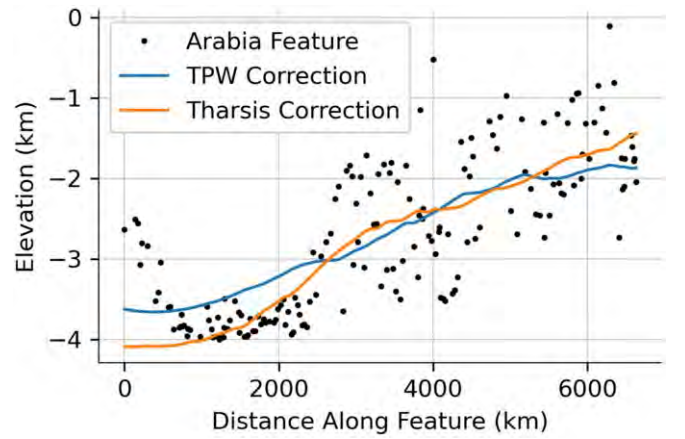

Figure 1. Arabia level elevation plotted against the approximate distance along the feature, with the Tharsis and TPW ($T_e = 200$ km) corrections. By comparison with Figure 1(b) of Citron et al. (2018) and Figure 1(b) of Perron et al. (2007), this figure validates our reproduction of the topographic corrections.

In the TPW scenario, deformation in response to reorientation of the planet is expressed by

$$\Lambda(\theta, \phi) = \frac{1}{3}\omega^2 R^2 [P_{2,0}(\cos\gamma) - P_{2,0}(\cos\theta)], \quad (1)$$

$$\Delta T(\theta, \phi) = \frac{\Lambda(\theta, \phi)}{g}[h_f - (1 + k_f)], \quad (2)$$

where $\Delta T(\theta, \phi)$ is the topographic change, g is the surface gravity, h_f and k_f are the secular (fluid-limit) degree-2 Love numbers that depend on the density and elastic structure of Mars, ω is the rotation rate, $P_{2,0}$ is the unnormalized degree-2 Legendre polynomial, γ is the angular distance between the deformation point and paleopole, θ is the colatitude, and ϕ is the longitude. For a range of lithosphere elastic thicknesses T_e, Perron et al. (2007) computed parameters that minimized the Arabia feature's reconstructed elevation variation. They primarily discuss results for $T_e = 200$ km, citing estimates for modern Mars, although higher values yield marginally better fits. The previously mentioned short-wavelength elevation scatter causes a large rms error for all values of T_e, so it is not clear that any one value of T_e is best. For each value of T_e, sea level is the vertical offset of the topographic correction that best matches the elevation of the Arabia feature. Figure 2(a) shows our reproduced global topographic change in response to the proposed TPW for $T_e = 200$ km.

In the TPW scenario, the Arabia level is formed after most of Tharsis is constructed. The relative timing is inferred from the location of best-fit paleopoles for the Arabia and Deuteronilus levels. Because the mass of Tharsis would resist reorientation away from the equator, post-Tharsis TPW would be constrained to the great circle roughly 90° from Tharsis. Indeed, best-fit paleopoles for both levels lie very close to this great circle, implying wander after the rise of Tharsis (Perron et al. 2007).

Unlike in the TPW scenario, the topographic correction in the Tharsis growth scenario is independent of the Arabia feature's mapped elevation. In the TPW scenario, model parameters were chosen to minimize the elevation variation of the Arabia level. In the Tharsis growth scenario, the topographic correction does not depend on the Arabia
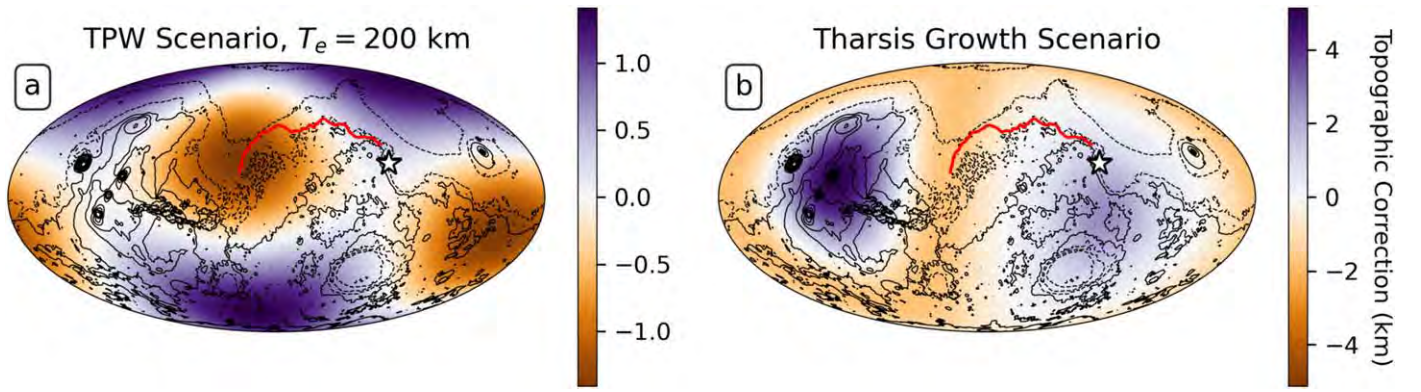
Figure 2. Global topographic corrections in the (a) TPW scenario with $T_e = 200$ km (Perron et al. 2007) and (b) Tharsis growth scenario (Matsuyama & Manga 2010; Citron et al. 2018). The white star indicates the location of Jezero crater. The red line traces the Arabia level as shown in Perron et al. (2007) and Citron et al. (2018). Black contours show modern Martian topography with 2 km intervals.

mapping. The deformation simply happens to correct the elevation variation roughly as well as the TPW models. However, like in the TPW scenario, sea level for the Tharsis growth scenario is the vertical offset that best aligns the topographic correction with mapped elevations.

In the Tharsis growth scenario, Matsuyama & Manga (2010) used the Martian gravity field to model the global topographic contribution of Tharsis. Citron et al. (2018) then subtracted this contribution from modern Martian topography to correct the Arabia level's elevation trend. The Tharsis contribution is expressed in terms of spherical harmonics,

$$\Delta T(\phi, \theta) = \sum_{n=0}^{N} \sum_{m=-n}^{n} (S_n^m - RG_n^m) Y_n^m(\theta, \phi), \qquad (3)$$

where N is the maximum degree of the spherical harmonic expansion (5 in this case), Y_n^m is the spherical harmonic of degree n and order m, S_n^m is the coefficient for Tharsis' contribution to the shape of Mars, G_n^m is the coefficient for Tharsis' contribution to the geoid of Mars, and R is the mean radius of Mars. Figure 2(b) shows our reproduced global topographic contribution of Tharsis.

In the Tharsis growth scenario, the Arabia level must form before or during the early stages of Tharsis emplacement, which is thought to have initiated >3.7 Ga (Anderson et al. 2001). Citron et al. (2018) propose that the Arabia level formed at least 4 Ga, in the Early Noachian, and suggest that the ocean was present during valley network formation. This would make the Arabia level one of the oldest recognizable features on the surface of Mars, as the basin impacts of Hellas, Argyre, and Isidis also occurred roughly at 4 Ga (Werner 2008; Fassett & Head 2011).

It is important to note that several inconsistent definitions of the Arabia level have appeared in prior studies (Sholes et al. 2021) and the TPW scenario and the Tharsis Growth scenario consider only one such definition. Their definition is borrowed from Carr & Head (2003), who relied on a generalized and interpolated version of the definition in Clifford & Parker (2001), which is based on an earlier abstract that does not appear to have figures or mapping associated with it at this time (Parker 1998). Further, both scenarios use an incomplete version of this definition (reproduced in Figure 2) to fit their correction models, ignoring segments of the mapping that appeared in prior studies. We will discuss the implications of this further in Section 5.

3. Jezero Crater

The Mars 2020 Perseverance rover is currently investigating Jezero crater, located at 18°.4 N, 77°.7 E on the western rise of the Isidis basin. It contains exceptionally well-preserved remnants of a fluvio-deltaic environment where two valley networks emptied into the crater from the west and north, forming an open-basin lake that was drained by an outlet canyon to the east (Fassett & Head 2005; Schon et al. 2012). Visually striking delta deposits lie at the mouths of the inlet valleys and are primary targets for in situ investigation by Mars 2020 (Schon et al. 2012; Goudge et al. 2017, 2018). Carbonate minerals are exposed in the fans and surrounding terrain, making Jezero a very rare location on Mars with this combination of morphology and mineralogy exposed at the surface (Ehlmann et al. 2009; Mustard et al. 2009; Goudge et al. 2015; Horgan et al. 2020).

Crater counting of the valley network system draining into Jezero indicates that fluvial activity ceased by 3.83 Ga, around the Noachian–Hesperian boundary (Fassett & Head 2008b) and consistent with the timing of global valley network formation (Howard et al. 2005; Irwin et al. 2005; Fassett & Head 2008b; Hynek et al. 2010; Goudge et al. 2016). This makes features in the Jezero crater paleolake appreciably older than many lacustrine features in Gale crater, which appear to have formed considerably later in Martian hydrological history. The antiquity of Jezero's features gives an unprecedented opportunity to link interpretations of local environments there to the global hydrology and climate on early Mars.

Figure 3 shows the application of the TPW and Tharsis growth corrections (Figure 2) to Jezero crater and its surroundings. The topographic deformation models are subtracted from regional topography. Then the corrected elevations are shown relative to the sea level proposed for each model, which is −2.3 km for the Tharsis growth scenario and −2.25 km for the TPW scenario (using $T_e = 200$ km). In the Tharsis growth scenario, the crater floor would be submerged under nearly 2 km of water, the outlet canyon would be more than 1 km underwater, and the nearest shore would be about 100 km west of Jezero. With the corrected topography, sea level could not have been above roughly −3.3 km without submerging the outlet canyon and flooding the crater (in its current form). The TPW correction submerges Jezero less than the Tharsis growth correction. For $T_e = 200$ km and its associated sea level of −2.25 km, the crater's elevation drops by about 180 m and the top of the outlet canyon is about 300 m
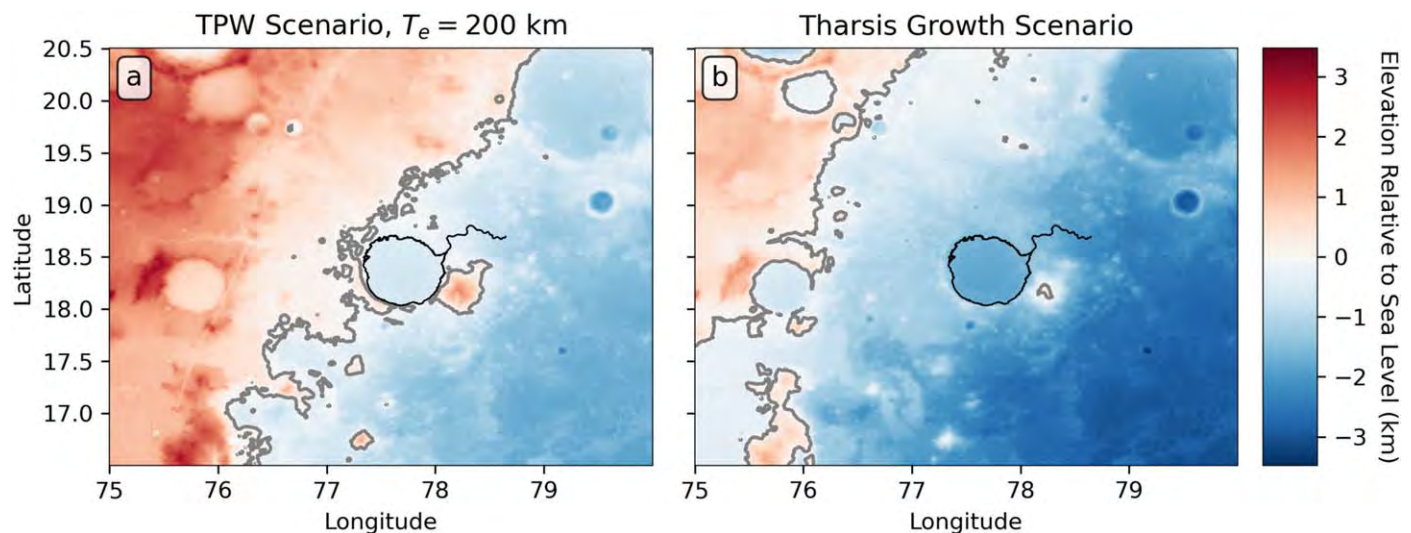
Figure 3. Topography of the region surrounding Jezero after applying the global elevation corrections due to (a) TPW with $T_e = 200$ km (Perron et al. 2007) and (b) Tharsis (Citron et al. 2018). The surface elevation is expressed relative to sea level (defined by the Arabia level best-fit elevation) in each scenario and the gray line traces sea level. Sea level is -2.25 km in the TPW scenario with $T_e = 200$ and -2.3 km in the Tharsis growth scenario. The black lines show the outlet canyon and the outline of the lake that it drained (Fassett & Head 2005; Goudge et al. 2019).

underwater, limiting sea level to roughly -2.55 km without flooding the crater. However, this is not the case for all the reported elastic thicknesses. For $T_e = 100$ km, the crater barely remains above sea level, but most of the outlet canyon is still submerged (see Figure 4(a)).

In both the TPW and Tharsis growth, Jezero is tilted slightly, in addition to the change in elevation. In both cases, the tilt is mainly in the north–south direction. In the TPW scenario, the northern side of the crater is lowered about 10 m more than the southern side. In the Tharsis growth scenario, the tilt is the other direction, lowering the southern side of the crater about 40 m more than the northern side. Although small, such tilting may be important for understanding the sedimentary architecture and stratigraphy in Jezero.

4. Implications

Based on these results, we conclude that fluvio-lacustrine activity at Jezero could not have coincided with the Arabia ocean in the Tharsis growth scenario. With pre-Tharsis topography, Jezero is unequivocally and deeply submerged by the ocean, inconsistent with observations of the inlet valley networks, deltas, and outlet canyon at Jezero, which could not have formed beneath hundreds of meters of water. More broadly, this conclusion suggests that a pre-Tharsis Arabia ocean did not exist during the main era of global valley network formation in the Noachian/Early Hesperian, which was coeval with the formation of the Jezero paleolake system (Howard et al. 2005; Irwin et al. 2005; Fassett & Head 2008b; Hynek et al. 2010).

In the Tharsis growth scenario, it is possible that the Arabia ocean entirely predates fluvio-lacustrine activity at Jezero. This requires the ocean to have substantially receded, most of Tharsis to have formed, or some combination of the two before valley network formation at Jezero. However, it is unlikely that the Arabia level is older than the basin impacts. The same authors who dated the cessation of fluvial activity at Jezero later computed ages near 4 Gyr for Hellas, Isidis, and Argyre (Fassett & Head 2011), although the timing of these basin impacts is uncertain and may be considerably earlier

Morbidelli et al. (2018). These impacts are estimated to have deposited 347, 212, and 34 m of material globally (Toon et al. 2010), which would have obscured the Arabia level. An older level is also more likely to be obscured by smaller impacts, erosion, and volcanism. However, we focus on the basin impacts because they are temporally constrained events with global implications.

If we assume that, at minimum, all or part of the putative Arabia shoreline could not have survived the basin impacts in recognizable form, we can estimate the window of time between basin impacts and fluvial activity at Jezero when the putative Arabia ocean may have existed. The oldest basin impact, Hellas, is thought to have occurred at approximately 4.04 Ga. The youngest, Argyre, is though to have occurred at approximately 3.94 Ga. In both cases, crater counting uncertainty is $\sim$10 Myr (Fassett & Head 2011). Fluvial activity at Jezero is estimated to have ceased by 3.83 Ga (Fassett & Head 2008b) and is statistically uncertain to 100 Myr. Therefore, it appears that a window of $\sim10^8$ yr exists between the basin impacts and the end of fluvial activity when the Arabia ocean could have existed. However, 3.83 Ga marks the end of fluvial activity at Jezero, not the beginning. Additionally, all of these dates are derived from crater counting and the systematic uncertainty in impactor flux is much larger than the stated uncertainties for the basin impacts. A precise estimate of the time available for an Arabia ocean is not yet possible. With the information available, however, we estimate a range of $\sim10^8$ yr available for a pre-Tharsis Arabia ocean to exist at Jezero before fluvial activity occurred there. As noted above, if the proposed ocean existed during this window of time, some combination of Tharsis growth and ocean loss must have subsequently lowered sea level below the Jezero outlet canyon terminus.

If the proposed ocean existed during a $\sim10^8$ yr window of time after the basin impacts, marine/coastal sediment or altered seafloor could have formed throughout the submerged terrain. If the Jezero impact occurred before the ocean waned, these units would drape the crater and be buried beneath the deltas in Jezero. The "mottled terrain" appears to be the only unit found
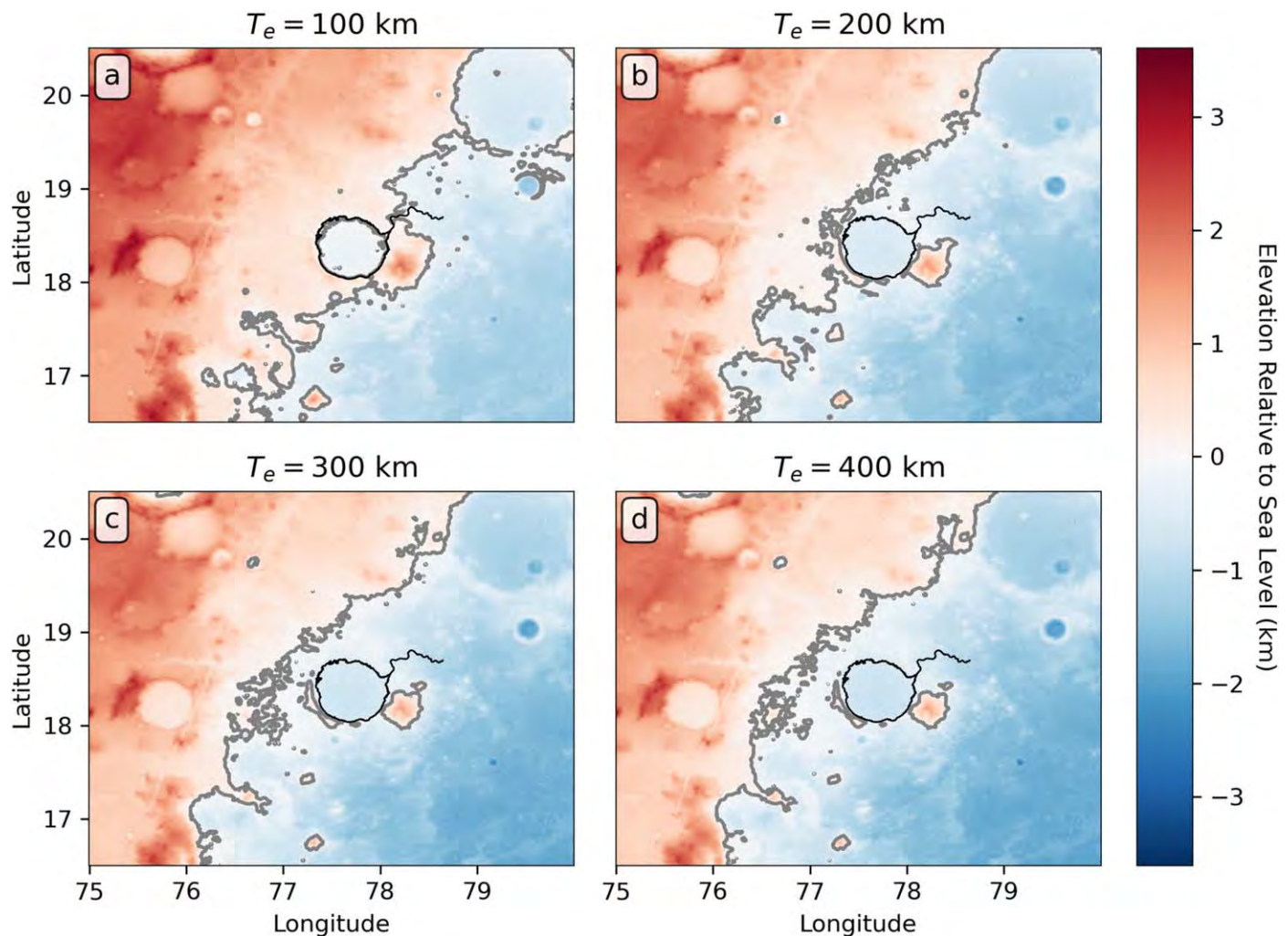
Figure 4. Topography of the region surrounding Jezero after applying the global TPW correction with different T_e values of (a) 100 km, (b) 200 km, (c) 300 km, and (d) 400 km, using parameters reported in Table 1 of Perron et al. (2007). The best-fit sea level in each of these cases is −2.55, −2.25, −2.15, and −2.15 km, respectively. The surface elevation is expressed relative to sea level (defined by the Arabia level best-fit elevation) in each scenario and the gray line traces sea level. The black lines show the outlet canyon and the outline of the lake that it drained (Fassett & Head 2005; Goudge et al. 2019). Higher T_e values submerge Jezero more deeply and yield marginally better fits to the Arabia level. For $T_e = 100$ km, although the crater is slightly above sea level, most of the outlet canyon is submerged.

under the delta outcrop and throughout the region surrounding Jezero, but its provenance is not entirely clear (Goudge et al. 2015). It is a magnesium carbonate and olivine-rich unit draping underlying topography and exhibiting curious banding, similar to a regionally identified olivine-rich unit (Mustard et al. 2009). Kremer et al. (2019) interpret this regional unit as an ash-fall deposit, likely related to volcanism in the greater Syrtis–Isidis area. The mottled terrain has no clear connection to an ocean at this point and there is no observational evidence to support such a connection. Further work may preclude any relation to the hypothetically submerged area. However, it is perhaps the best place to look for such a connection, and the Perseverance rover will have the opportunity to explore this unit in situ.

For the same reasons as discussed for the Tharsis growth scenario, it is also unlikely that fluvio-lacustrine activity at Jezero coincided with the Arabia ocean of the TPW scenario. The TPW corrections submerge Jezero for values of T_e more than about 200 km and these higher T_e values yield marginally better fits. Even for $T_e = 100$ km, most of the outlet canyon is submerged (see Figure 4(a)). The later timing of the ocean in this scenario, after most of Tharsis forms, may require the

ocean to appear after cessation of fluvial activity at Jezero. This is problematic for reasons discussed next for both scenarios.

An Arabia ocean after hydrological activity at Jezero is doubtful in both the Tharsis growth and TPW scenarios for a few reasons. First, satellite data show no sign of marine or coastal sediment overlying the deltas in the crater (Goudge et al. 2015), although we will learn much more about the stratigraphy in Jezero during the Perseverance rover's mission. Second, this would require an improbable transition from a climate sustaining valley network formation but no large ocean to another with a large ocean but not enough valley network activity to reset the cessation ages. Further modeling of water inventory evolution and 3D climate could yield insight into the likelihood of such a transition occurring.

5. Discussion and Conclusion

We have linked global topographic corrections used to flatten the proposed Arabia level to the geology and environmental history at Jezero crater. In the Tharsis growth scenario, the Arabia ocean would submerge Jezero and its surroundings under more than 1 km of water. This precludes

the simultaneous existence of the proposed ocean and fluvio-deltaic activity at Jezero. Based on crater counting, it also implies that the proposed Arabia ocean did not exist during the main era of global valley network incision in the Noachian/Early Hesperian. The same argument applies to the TPW scenario, where most values of T_e submerge Jezero. In the Tharsis growth scenario, there are $\sim 10^8$ yr between the basin impacts and the end of fluvial activity at Jezero when the Arabia ocean could have existed. In this case, some combination of ocean loss and Tharsis growth must occur before fluvio-lacustrine activity at Jezero.

Although we describe the timing of these events as precisely as possible given current information, we are cognizant of the considerable uncertainty in the timeline. Some recent work suggests that fluvial activity at Jezero could have occurred considerably later than most estimates (Mangold et al. 2020), which would increase the hypothetical window of time available for the proposed ocean. More precise construction of the timeline at Jezero crater may be possible after samples are returned to Earth for geochronological analysis.

Before then, the possibility that any features in Jezero are marine in origin could potentially be determined by the Perseverance rover and further scrutiny of orbital data. To our knowledge, the "mottled terrain" is the only unit with a stratigraphic and spatial context that could plausibly be linked to an ancient ocean, but there is no evidence to support such a link at this time. Future work examining this unit, either with orbital data or in situ, could evaluate any possible connection. Future work could also assess the likelihood that the proposed Arabia shoreline could survive impact gardening and other processes after the basin impacts. Finally, although several studies have attempted to rectify the topographic variation of putative shoreline features on Mars, few have sought to examine the features in detail or constrain the age of shoreline bearing terrain (Sholes et al. 2019b, 2021). More direct estimates of proposed shoreline ages could anchor them in the timeline of events discussed here.

More complex topographic deformation models could modify the results presented here. Future models could include spatially and temporally variable elastic lithospheric thickness, for example, or the effect of more localized volcanic and sedimentary loads. In the Tharsis growth scenario, Jezero elevation would need to increase about 1 km to bring it out of the ocean. In the TPW scenario, hundreds of meters are required to avoid submerging the outlet canyon. Future models must consider the timing of basin impacts, Tharsis growth, potential TPW, hydrological activity, and more localized topographic deformation mechanisms in a self-consistent manner. Post-basin loading of Isidis (Citron et al. 2021), in particular, appears to be an important consideration.

However, future models must also contend with the inconsistency of the shoreline definitions instead of relying on one segment of a single, questionable definition (see Section 2). We have explored the consequences of two influential correction scenarios, but the consequences may be different with a better treatment of the uncertain shoreline locations and improved understanding of the features more generally. Future work addressing how different shoreline definitions influence the topographic correction scenarios should soon be possible with newly available, digital versions of the many definitions (Sholes et al. 2021).

Finally, future work could constrain the timing and extent of possible oceans on Mars by examining other sites around the dichotomy. By characterizing the geology of reasonably well dated sites at the right locations, it may be possible to assemble firm constraints on the maximum size of oceans at various points in Martian history. A broader study like this would account for different topographic deformation models and, if feasible, likely sources of more local deformation.

ORCID iDs

Mark Baum ⓘ https://orcid.org/0000-0001-8832-4963
Robin Wordsworth ⓘ https://orcid.org/0000-0003-1127-8334
Timothy A. Goudge ⓘ https://orcid.org/0000-0003-4297-9838

References

Anderson, R. C., Dohm, J. M., Golombek, M. P., et al. 2001, JGR, 106, 20563
Baum, M. 2021a, wordsworthgroup/jezero-shoreline-deformation v1.1, Zenodo, doi:10.5281/zenodo.4728201
Baum, M. 2021b, Wordsworthgroup/orthopoly v0.9.1, Zenodo, doi:10.5281/zenodo.4430584
Bishop, J. L., Fairén, A. G., Michalski, J. R., et al. 2018, NatAs, 2, 206
Bouley, S., Baratoux, D., Matsuyama, I., et al. 2016, Natur, 531, 344
Carr, M. H., & Head, J. W. 2003, JGRE, 108, 5042
Chan, N.-H., Perron, J. T., Mitrovica, J. X., & Gomez, N. A. 2018, JGRE, 123, 2138
Citron, R. I., Manga, M., & Hemingway, D. J. 2018, Natur, 555, 643
Citron, R. I., Manga, M., Hemingway, D., & Plattner, A. 2021, LPSC, 52, 1605
Clifford, S. M., & Parker, T. J. 2001, Icar, 154, 40
Daradich, A., Mitrovica, J. X., Matsuyama, I., et al. 2008, Icar, 194, 463
Di Achille, G., & Hynek, B. M. 2010, NatGe, 3, 459
Ehlmann, B. L., & Edwards, C. S. 2014, AREPS, 42, 291
Ehlmann, B. L., Mustard, J. F., Murchie, S. L., et al. 2011, Natur, 479, 53
Ehlmann, B. L., Mustard, J. F., Swayze, G. A., et al. 2009, JGR, 114, E00D08
Fassett, C. I., & Head, J. W. 2005, GeoRL, 32, L14201
Fassett, C. I., & Head, J. W. 2008a, Icar, 198, 37
Fassett, C. I., & Head, J. W. 2008b, Icar, 195, 61
Fassett, C. I., & Head, J. W. 2011, Icar, 211, 1204
Forget, F., Wordsworth, R., Millour, E., et al. 2013, Icar, 222, 81
Goudge, T. A., Fassett, C. I., Head, J. W., Mustard, J. F., & Aureli, K. L. 2016, Geo, 44, 419
Goudge, T. A., Fassett, C. I., & Mohrig, D. 2019, Geo, 47, 7
Goudge, T. A., Milliken, R. E., Head, J. W., Mustard, J. F., & Fassett, C. I. 2017, E&PSL, 458, 357
Goudge, T. A., Mohrig, D., Cardenas, B. T., Hughes, C. M., & Fassett, C. I. 2018, Icar, 301, 58
Goudge, T. A., Mustard, J. F., Head, J. W., Fassett, C. I., & Wiseman, S. M. 2015, JGRE, 120, 775
Grant, J. A., & Parker, T. J. 2002, JGRE, 107, 5066
Grotzinger, J. P., Gupta, S., Malin, M. C., et al. 2015, Sci, 350, aac7575
Grotzinger, J. P., Sumner, D. Y., Kah, L. C., et al. 2014, Sci, 343, 1242777
Head, J. W., Forget, F., Wordsworth, R., et al. 2018, LPSC, 49, 2194
Head, J. W., Hiesinger, H., Ivanov, M. A., et al. 1999, Sci, 286, 2134
Hoke, M. R., Hynek, B. M., & Tucker, G. E. 2011, E&PSL, 312, 1
Horgan, B. H., Anderson, R. B., Dromart, G., Amador, E. S., & Rice, M. S. 2020, Icar, 339, 113526
Howard, A. D., Moore, J. M., & Irwin, R. P. 2005, JGRE, 110, E12S14
Hunter, J. D. 2007, CSE, 9, 90
Hynek, B. M., Beach, M., & Hoke, M. R. T. 2010, JGRE, 115, E09008

Irwin, R. P., Howard, A. D., Craddock, R. A., & Moore, J. M. 2005, JGRE, 110, E12S15

Irwin, R. P., III, Maxwell, T. A., Howard, A. D., Craddock, R. A., & Leverington, D. W. 2002, Sci, 296, 2209

Kasting, J. F. 1991, Icar, 94, 1

Kremer, C. H., Mustard, J. F., & Bramble, M. S. 2019, Geo, 47, 677

Leverington, D. W., & Ghent, R. R. 2004, JGRE, 109, E01005

Malin, M. C., & Edgett, K. S. 1999, GeoRL, 26, 3049

Malin, M. C., & Edgett, K. S. 2003, Sci, 302, 1931

Mangold, N., Dromart, G., Ansan, V., et al. 2020, AsBio, 20, 994

Matsuyama, I., & Manga, M. 2010, JGRE, 115, E12020

Moore, J., & Wilhelms, D. E. 2001, Icar, 154, 258

Morbidelli, A., Nesvorny, D., Laurenz, V., et al. 2018, Icar, 305, 262

Mustard, J. F., Ehlmann, B. L., Murchie, S. L., et al. 2009, JGRE, 114, E00D12

Niles, P. B., Catling, D. C., Berger, G., et al. 2013, SSRv, 174, 301

Palucis, M. C., Dietrich, W. E., Williams, R. M. E., et al. 2016, JGRE, 121, 472

Parker, T. J. 1998, LPSC, 29, 1965

Parker, T. J., Gorsline, D. S., Saunders, R. S., Pieri, D. C., & Schneeberger, D. M. 1993, JGR, 98, 11061

Parker, T. J., Stephen Saunders, R., & Schneeberger, D. M. 1989, Icar, 82, 111

Perron, J. T., Mitrovica, J. X., Manga, M., Matsuyama, I., & Richards, M. A. 2007, Natur, 447, 840

Roberts, J. H., & Zhong, S. 2007, Icar, 190, 24

Ruiz, J., Fairén, A. G., Dohm, J. M., & Tejero, R. 2004, P&SS, 52, 1297

Schon, S. C., Head, J. W., & Fassett, C. I. 2012, P&SS, 67, 28

Sholes, S. F., Catling, D. C., Pretlow, R., & Montgomery, D. R. 2014, LPICo, 1791, 1014

Sholes, S. F., Dickeson, Z. I., Montgomery, D., & Catling, D. 2021, JGRE, 126, e06486

Sholes, S. F., Montgomery, D. R., & Catling, D. C. 2019a, LPICo, 2089, 6282

Sholes, S. F., Montgomery, D. R., & Catling, D. C. 2019b, JGRE, 124, 316

Soto, A., Mischna, M., Schneider, T., Lee, C., & Richardson, M. 2015, Icar, 250, 553

Steakley, K., Murphy, J., Kahre, M., Haberle, R., & Kling, A. 2019, Icar, 330, 169

Toon, O. B., Segura, T., & Zahnle, K. 2010, AREPS, 38, 303

Turbet, M., & Forget, F. 2019, NatSR, 9, 5717

Urata, R. A., & Toon, O. B. 2013, Icar, 226, 229

Werner, S. 2008, Icar, 195, 45

Williams, R. M. E., Grotzinger, J. P., Dietrich, W. E., et al. 2013, Sci, 340, 1068

Wordsworth, R. 2016, AREPS, 44, 381

Wordsworth, R., Forget, F., & Eymet, V. 2010, Icar, 210, 992

Wordsworth, R., Forget, F., Millour, E., et al. 2013, Icar, 222, 1